Functional Materials 16, No.4 (2009)

Superlattice nanostructures based on chalcogenide semiconductors

A.Yu.Sipatov

National Technical University "Kharkiv Polytechnical Institute",
21 Frunze St., 61002 Kharkiv, Ukraine

Received September 15, 2009

The multilayer chalcogenide semiconductor films with large layer lattice misfit (0.5–13 %) are shown to open the new opportunities for development of one-, two- and three-dimensional superlattice nanostructures. The superconductivity has been revealed for the first time in two-dimensional (dislocational) superlattices, the presence of periodic networks of misfit dislocations at interfaces being directly responsible for the superconductivity. The spectra of luminescence from quantum dots have been discovered for the first time in three-dimensional PbSe–PbS superlattices, the dots being formed by structure modulations from periodic misfit dislocations along the layer interfaces and composition modulations in the orthogonal direction. The resonance tunneling of electrons via ferromagnetic EuS barriers was found for one-dimensional (compositional) superlattices. The antiferromagnetic interlayer coupling of magnetic EuS layers via non-magnetic PbS and YbSe spacers has been found for the first time in semiconductor superlattices. Such coupling is observed for unusual wide range of spacer thicknesses for narrow-gap PbS semiconductor (from 0.4 nm to 40 nm) and wide-gap YbSe (from 1 nm to 3 nm).

Показано, что использование многослойных пленок халькогенидных полупроводников с несоответствием решеток соседних слоев в широких пределах (0,5–13 %) открывает новые возможности по созданию одно-, двух- и трехмерных сверхрешеточных наноструктур. Для двумерных (дислокационных) сверхрешеток впервые обнаружена сверхпроводимость, которая связана с присутствием периодических сеток дислокаций несоответствия на межфазных границах (отсутствие дислокаций приводит к отсутствию сверхпроводимости). Для трехмерных сверхрешеток PbSe–PbS впервые обнаружены спектры люминесценции из квантовых точек, созданных модуляцией структуры периодическими дислокациями вдоль межфазных границ и модуляцией состава в ортогональном направлении. Для одномерных (композиционных) сверхрешеток обнаружено резонансное туннелирование электронов через ферромагнитные барьеры EuS, а также антиферромагнитное упорядочение магнитных слоев, обусловленное их взаимодействием через диамагнитные прослойки PbS и YbSe. Такое упорядочение наблюдается для необычно большого диапазона толщины прослоек узкозонного полупроводника PbS (0,4–40 нм) и широкозонного YbSe (1–3 нм).

The main goal of materials science is to synthesize new materials and to study the structure and properties thereof. It is just the superlattices (SLs) that are among the most promising objects. The SLs are multilayered structures with periodically alternating superthin layers of different materials providing an additive modulating potential for charge carriers [1]. The SLs are of a great interest both in fundamental studies and in practical applications. The main requirements in development of epitaxial SLs are as follows: (i) the layer-by-layer alternating growth of the materials in use, (ii) a difference in the band gaps thereof; (iii) a small misfit between their lattice periods. The largest progress is achieved for the A^3B^5 and A^2B^6 SLs where the small lattice

misfit is provided by multicomponent barrier layers. An insufficient attention was given to multilayer structures with a large lattice misfit, as the misfit was assumed to cause stresses, strains, and defects resulting in additional scattering centers of charge carriers. The development of such SLs and studies of the physical properties thereof will make it possible to extend considerably the variety of superlattice materials of practical interest, while the lattice misfit offers new ways to SLs with homogeneously and inhomogeniously elastically strained layers, ordered dislocation systems, and coincidence site lattice at the interfaces. This will extend considerably both the number of structure states and thus the variation ranges of the SL physical properties.

The binary chalcogenide semiconductors were selected as the study objects, see Table 1. Those have a simple crystal lattice of NaCl type, are rather simple to obtain as single crystal films on various substrates (KCl, BaF_2, mica, Si), show a wide lattice misfit range (f = 0.5 to 15 %), and provide the formation of multilayered compositions with different layer combinations (narrow-gap, wide-gap, ferromagnetic and nonferromagnetic, etc.).

To resolve the problem, an original high-vacuum unit was designed providing the oil-free pumping system (down to 10^{-7} Pa), the resistive evaporation of lead and tin chalcogenides from tungsten boats and electron-beam evaporation of rare-earth metal (REM) chalcogenides. The multilayered films were synthesized by successive condensation of the chalcogenides onto freshly cleaved KCl and BaF_2 substrates at 200–250°C. The

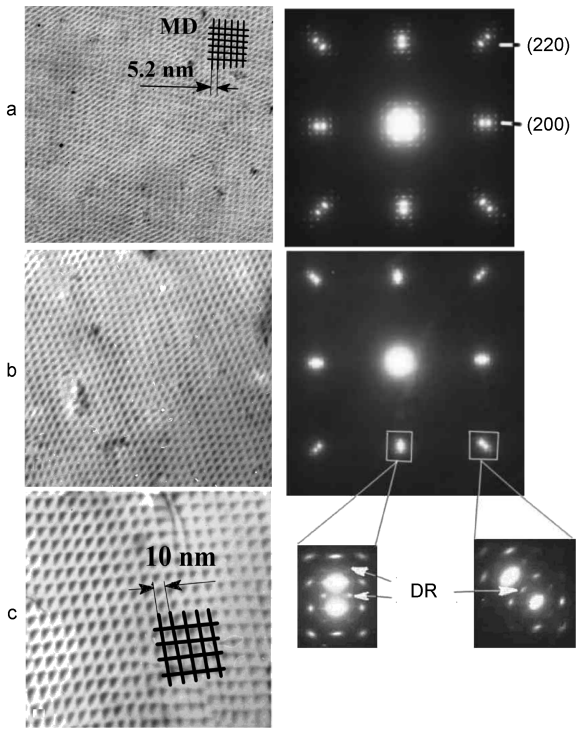

Fig. 1. Electron microscopic images (left) and electron diffraction patterns (right) of YbS–PbSe (a), YbS–PbS (b) and YbSe–PbSe (c) films. Dislocation reflections are denotd as DR.

layer thickness and the condensation rate were monitored by a calibrated quartz resonator placed near the substrates. Modern methods of high-resolution electron microscopy, X-ray and neutron diffraction were used in structure studies; a set of modern low-temperature methods was used to examine the optical, electrical, and magnetic characteristics of the films.

Table 1. Lattice periods (a), heat expansion coefficients (α), band gap widths (E_g), melting points (T_m), Curie points (T_C), and Neel temperatures (T_N) for materials studied

Materials	a, nm	$\alpha_{(300K)}\cdot 10^{-6}$, deg^{-1}	E_g (300 K), eV	T_m, °C	T_C, K (T_N), K
PbS	0.5936	20.3	0.41	1113	—
PbSe	0.6126	19.4	0.29	1080	—
PbTe	0.645	19.8	0.32	923	—
SnTe	0.633	20.8	0.18	806	—
YbS	0.5658	16	1.7	2230	—
YbSe	0.5879	17	2.0	2210	—
YbTe	0.6366	18	1.9	1930	—
EuS	0.5965	16.2	1.65	2560	16.5
EuSe	0.6188	18.6	1.8	2213	2.8 (4.6)
EuTe	0.6585	18	2.0	1983	(9)

Table 2. Calculated (f, D) and experimental (h_c, h_m) parameters of superlattices: f is the lattice misfit of the layers; D_{MD}, the MD period; h_c, the critical layer thickness for MD introduction; h_m, the minimum layer thickness for SL formation

SL	f, %	D_{MD}, nm	h_c, nm	h_m, nm
EuS–PbS	0.5	–	–	0.6
YbTe–SnTe	0.6	–	–	0.8
EuSe–PbSe	0.9	–	–	1.0
YbSe–PbS	0.9	–	–	1.0
EuTe–PbTe	2.0	23	8	1.2
PbTe–SnTe	2.1	23	7.5	1.4
EuS–PbSe	2.5	20	7	1.5
PbSe–PbS	3.1	13	6	1.5
SnTe–PbS	3.3	13	6	1.6
EuSe–PbS	4.0	12	5	1.8
YbSe–PbSe	4.1	10	4.5	2.0
EuSe–PbTe	4.4	10	4	2.0
YbS–PbS	4.8	8.5	3	2.0
PbTe–PbSe	5.3	8.4	3	2.0
EuTe–PbSe	7.2	6.2	2	3.0
EuS–PbTe	7.7	5.7	1	3.0
YbS–PbSe	7.9	5.2	1	3.5
PbTe–PbS	8.3	5.2	1	3.5
YbSe–PbTe	9.2	4.7	1	4.0
EuTe–PbS	10.0	4.3	1	4.0
YbS–PbTe	13.0	3.3	1	4.0

A SL should consist of sufficient good quality single-crystal layers to provide the most full realization of its unique properties. As to lead and tin chalcogenides, the KCl and BaF_2 substrates are known to be the optimal, where the single crystal films grow in (001) and (111) orientation, respectively. A study of the REM chalcogenide epitaxy has shown that those grow as polycrystalline films, at best as textured ones. The single-crystal layers of REM chalcogenides have been obtained using the lead and tin chalcogenide films where the required films grow in a layer-by-layer manner according to the Franck-van der Merve mechanism resulting in formation of the single-crystal films with at least the same crystal structure perfection as the substrate one. At a lattice misfit $f > 2$ %, a square network of pure edge misfit dislocations (MDs) is formed at the (001) interfaces. The MDs provided the compensation of the lattice misfit between the conjugated layers and localization of stresses and strains caused by that misfit near the interface in the form of periodic modulations. The dislocation-induced stresses are quite sufficient to modulate the semiconductor band gap. Taking into account the high regularity and periodicity of the MDs (where the electron diffraction is observed as dislocation reflects in the electron diffraction patterns), those can be considered as a new type of two-dimensional (dislocational) superlattices with a periodic structural modulation in the interface plane [2]. When varying the misfit value (from 13 to 2 %), the dislocation structures with a period from 3 nm to 30 nm can be obtained, Table 2.

In diffraction patterns of the multilayered structures, an interference pattern consisting of satellite reflections arises instead of the Bragg reflections from each material; the reflection spacing is defined by the multilayer period, Fig. 2a. A similar system of satellite peaks is observed for low angle X-ray scattering, too, Fig. 2b. Using the transmission X-Ray scattering, the layer thickness causing the pseudomorphism break (or a MD introduction) can be deter-

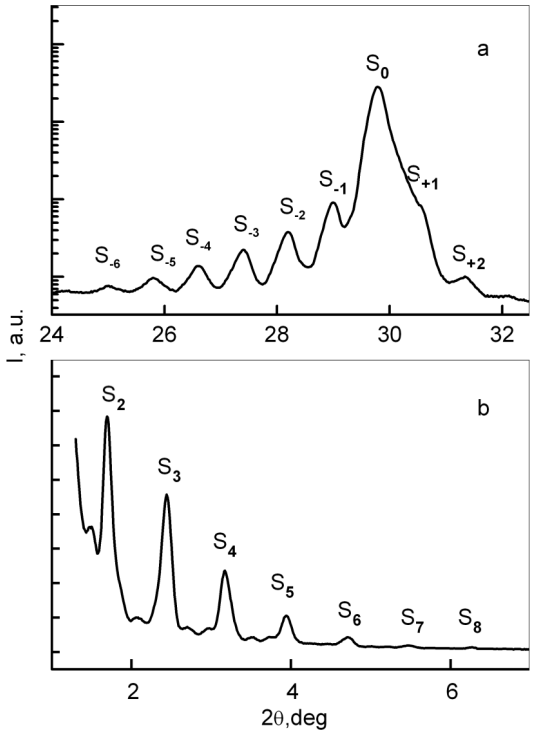

Fig. 2. X-ray diffraction patterns of an EuS–PbSe/(001)KCl SL with 11.4 nm period in the (200) reflection (a) and near the primary beam (b). Satellite reflections are denoted as S_n.

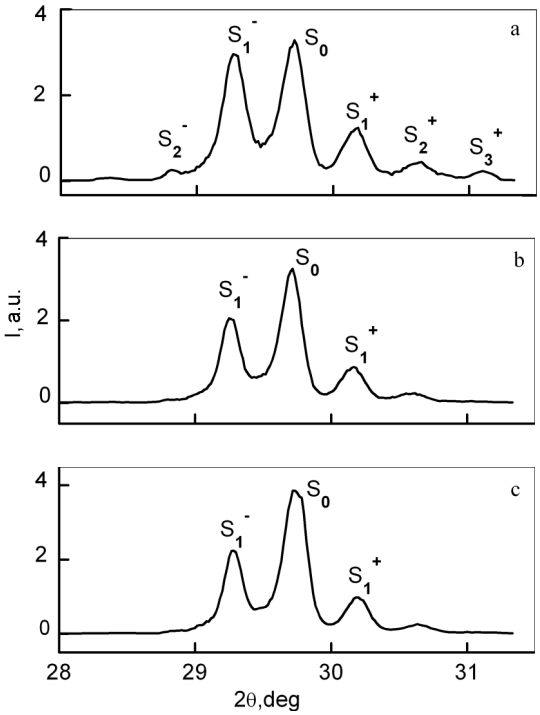

Fig. 3. X-ray diffraction in the (200) reflection of a PbSe–PbS SL with 22 nm period in the initial state (a) and annealed at 543 K for 10 h (b) and 78 h (c). Satellite reflections are denoted as S_n.

mined from the pseudomorhic reflection split into two separate ones corresponding to each layer. In this manner, the critical layer thickness for the MD formation was determined for each couple of the materials studied, the results are presented in Table 2. The Table presents also the minimal layer thickness values providing the possibility of superlattice formation, that thickness is determined from the presence of at least first order satellite reflections.

The structure study results can be summarized as follows. Basing on chalcogenide semiconductors, three types of superlattice nanostructures can be formed, namely (i) the one-dimensional (composition) SLs synthesized at small layer misfit and thickness being smaller than the critical ones for MDs; (ii) two-dimensional (dislocation) SLs at larger misfits and the layer thickness exceeding the critical ones for MDs; (iii) three-dimensional (composition-dislocation) SLs being a combination of two preceding ones.

A large concentration gradient over such small distances may cause a fast layer intermixing and the superlattice degradation even at the preparation stage. Therefore, the temperature and time stability studies of such nanostructures is among the matters of most importance. The effective methods of such studies include the X-ray diffraction making it possible to monitor the layer intermixing processes from the intensity changes of the satellite reflections as well as to determine the interdiffusion coefficients thereof [3–5]:

$$\ln\frac{I_m(t_2)}{I_m(t_1)} = -8\frac{\pi m^2}{H}D(t_2 - t_1), \qquad (1)$$

where I_m is the m-th satellite intensity normalized to the zero one; t_1 and t_2, the annealing time moments; m, the satellite order; H, the SL period; D, diffusion coefficint.

The SLs were subjected to diffusional annealings in vacuum at different temperatures. After each annealing, XRD patterns were obtained. The results are presented in Table 3 where the SLs studied are seen to be rather stable structures having in as-prepared state very small intermixed zone thickness ΔX ($\Delta X^2 \sim 4Dt$) of the order of one monolayer or less, thus being a very

Table 3. Diffusion characteristics of SLs: f is the lattice misfit of the layers; H, the SL period; h_i, layer thickness; T, the annealing temperature; D, diffusion coefficient; D_0, pre-exponential factor; E_a, activation energy; $D_{523\ K}$, diffusion coefficient at 523 K; ΔX, the intermixed zone thickness at 523 K for 1 h

SL	f, %	$H(h_1+h_2)$, nm	T, K	D, cm^2/s	D_0, cm^2/s	E_a, eV	$D_{523\ K}$, cm^2/s	ΔX, nm
PbSe–PbS	3.1	18 (9+9) 20 (14+6)	543	$1.6\cdot10^{-20}$	$5.3\cdot10^{-4}$	1.78	$1.6\cdot10^{-19}$	0.48
			593	$4\cdot10^{-19}$				
			623	$2.1\cdot10^{-18}$				
PbTe–PbSe	5.3	8.6 (4.3+4.3)	543	$2.3\cdot10^{-20}$	$1.6\cdot10^{-6}$	1.5	$5.6\cdot10^{-21}$	0.09
			593	$1.9\cdot10^{-19}$				
			643	$3.1\cdot10^{-18}$				
EuS–PbS	0.5	8.0 (4+4)	543	$1.1\cdot10^{-20}$	$2.2\cdot10^{-9}$	1.22	$3\cdot10^{-21}$	0.06
			593	$6.4\cdot10^{-20}$				
			623	$1.7\cdot10^{-18}$				
EuS–PbSe	2.5	19 (9.5+9.5)	593	$7.7\cdot10^{-21}$	$4.0\cdot10^{-10}$	1.26	$2.9\cdot10^{-22}$	0.02
		11.5 (10+1.5)	693	$3.3\cdot10^{-19}$				
		8.6 (6+2.6)	733	$8.7\cdot10^{-19}$				
EuSe–PbS	4.0	14 (7+7)	573	$0.8\cdot10^{-18}$	$1.1\cdot10^{-11}$	0.9	$2.2\cdot10^{-20}$	0.18
			598	$1.7\cdot10^{-18}$				
			623	$3.5\cdot10^{-18}$				
EuSe–PbSe	0.9	15 (8+7)	673	$0.5\cdot10^{-18}$	$9.9\cdot10^{-6}$	1.78	$7.5\cdot10^{-23}$	0.01
		13 (7+6)	698	$1.2\cdot10^{-18}$				
		16 (8+8)	723	$4.5\cdot10^{-18}$				
PbTe–PbS	8.3	Are not intermixed up to 750 K						
EuS–PbTe	7.7	Are not intermixed up to 750 K						

promising objects for further studies and search for new effects.

The dimensional quantization and resonance tunneling are effects typical of the SLs. The dimensional quantization can be revealed as separate emission lines corresponding to transitions between quantum levels (mini-bands) in the photoluminescence spectrum as well as changes in positions of those lines when varying the quantum well width and the pumping (excitation) levels. That has been demonstrated for the nanostructures obtained [6, 7]. In the dependences of the long-wave photoluminescence edge on the single-layer film thickness, its increase from 260 meV up to 500 meV is observed as the thickness is reduced from 30 nm to 3 nm. The experimental points agree well with the calculated position of the 1st dimensional quantization level for a single quantum well. A similar dependence is observed also for the EuS–PbS SL (Fig. 4) where the positions of experimental points agree well with the positions of the 1st and 2nd dimensional quantization levels calculated in the frame of Kronig-Penney model. The photoluminescence is of most interest in three-dimensionally modified structures, or dislocation-composition SLs, e.g., PbSe–PbS one [8]. The photoluminescence spectra (Fig. 5) contain four main equidistant lines, their positions are temperature-independent (within the temperature range of their existence). The temperature variation results in the intensity redistribution between those lines. At higher temperatures, the lines corresponding to higher energies become more intense. The positions of those four lines in the spectrum of the SL mentioned and especially the temperature independence thereof agree well with the dimensional quantization predictions in the quantum dot model.

Electrical Properties of Superlattices. Historically, the first reason for SL development was the prediction of unique elec-

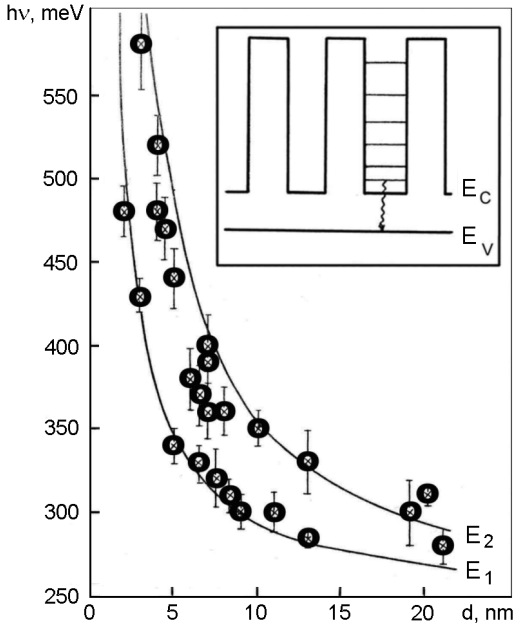

Fig. 4. Dependences of the long-wave edge of photoluminescence peaks for a EuS–PbS SL on the PbS layer thickness; E_i are calculated curves of the dimensional quantization level position. Inset: a schematic SL band model.

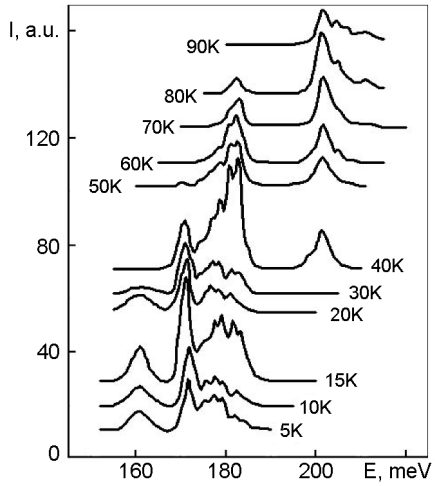

Fig. 5. Photoluminescence spectrum of a PbSe–PbS SL (each layer of 7 nm thickness) at temperatures from 5 K to 90 K.

trophysical peoperties thereof [1], in particular, of negative differential conductance, and of possible application thereof in GHz and THz range electronics. The nonlinearity of transport properties is especially pronounced at transversal transport (along the SL axis) where the charge carrier tunneling through the barrier layers occurs. That is why a special attention is given to the transversal transport and tunneling when studying the electrophysical properties of SLs.

The transversal transport studies in EuS–PbS multilayered structures have shown the presence of the electron resonance tunneling through thin (2 to 5 nm) EuS barriers, therefore, such structures have strongly nonlinear IVCs (Fig. 6) including sections with negative differential conduction (for two-barrier structures) [9–11]. The conductance of such structures has been found to change as when the barrier layers transit into the ferromagnetic state and the change sign is defined by the mutual orientation of magnetization in the neighboring EuS layers. Such conduction changes are connected with the exchange split of the barrier layer conduction band and the spin polarization of electrons tunneling therethrough. That is why such structure are very promising for the spintronics (the spin-polarized electronics) where not only the charge carrier current value but also the spin state thereof can be controlled.

When studying the longitudinal transport properties of SLs, the superconductivity (SC) of two-dimensional dislocation SLs was revealed in the multilayer PbTe–PbS structures [12–14] where there are no superconducting transitions in single-layer films. The SL superconductivity is connected with the presence of regular misfit dislocation networks at the interfaces (there is no superconductivity if the dislocation networks are absent) and has the following characteristics: the transition point T_c = 2–6.5 K; the maximum critical magtnetic field H_{c2} = 30–40 kOe, the energy gap (Δ) — $2\Delta/kT_c$ ~ 10.

The superconductivity of dislocation SLs is of two-dimensional character and is localized near the interfaces. The pairing of carriers occurs initially in the vicinity of the dislocation network sites (that is evidences by the occurrence of zero-dimensional fluctuation SC). The superconductivity is stabilized by the interaction of neighboring dislocation sites (the occurrence of two-dimensional fluctuation SC) and then of neighboring MD networks through the lead chalcogenide layer. The superconductivity observed in the dislocation SLs is nontrivial and is not explained by none of existing theories, for example, the temperature dependence of superconducting gap does not correspond to the Bardeen-Cooper-Schrieffer theory. A certain similarity in the crystal structure elements and the analogy in SC

Table 4. Lattice misfit (f), misfit dislocation period (D_{MD}), and maximum critical temperature of SC transition (T_c) for SLs

	SL	f	%	D_{MD}, nm
A	PbTe–SnTe	2.0	23	2.9
	PbSe–PbS	3.1	13.6	4.5
	PbTe–PbSe	5.1	8.6	6.02
	PbTe–PbS	8.3	5.2	6.53
B	YbS–PbS	4.8	8.5	5.39
	YbS–PbTe	13	3.3	5.93
C	EuS–PbSe	2.5	17	2.48
	EuS–PbTe	7.7	5.7	5.01
	EuS–PbS	0.5	No MD	No SC
D	YbS–YbSe	3.8	10.6	No SC
	YbS–EuS	5.3	7.7	No SC

properties of dislocation SLs and HTSC suggests a similarity of the superconductivity nature and mechanisms in such structures. The collection of the studies allows to conclude that the dislocation SLs are a convenient HTSC model [13] where the characteristic structure dimensions are one decimal order larger and the critical parameters are respectively decreased, thus, the study thereof is much simplified.

The superconductivity in two-dimensional dislocation SLs was revealed also for other multilayer structures including lead, tin, europium, and ytterbium chalcogenides, see Table 4 [15, 16].

When considering the effect of MD period on the SC transition temperature, it is to note that there are four different SL types noted in the Table as A, B, C and D. The type A SLs consist of narrow-band semiconductors only and show higher T_c values than other SL types. In the B type SLs, one of the layer materials is a wide-band semiconductor and thus the carrier concentration averaged over the SL is substantially lowered. Therefore, the T_c in such SLs is lower than that in the A type ones. In the C type SLs, one of the material (EuS) is a wide-band semiconductor and ferromagnetic. In such SLs, the T_c is lowered as compared to that of the preceding ones due to the proximity effect and the SC suppressing by the ferromagnetic. However, the supeconductivity is not vanished completely even in such SLs with ferromagnetic layers.

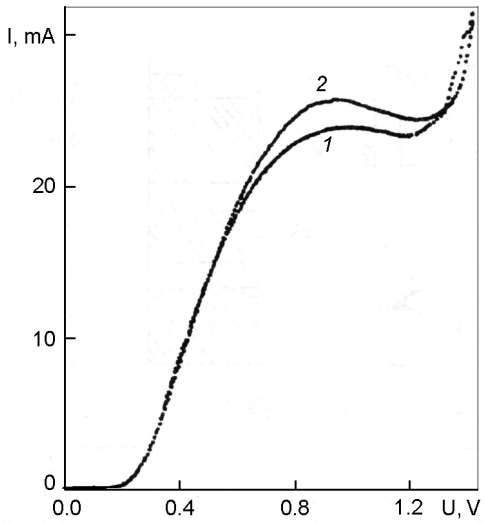

Fig. 6. IVC of the transversal transport for a two-barrier tunneling structure EuS(3 nm)–PbS(7 nm)–EuS(3 nm)/ (001)PbTe (the mesastructure section 100×100 μm) at 77 K obtained at the voltage increase (*1*) and decrease (*2*).

The dependence of the SC transition point on the MD period is to be considered individually for each SL type (Fig. 6). It is obviously at such consideration that the increasing MD density (shortening the MD period) results in elevation of the SC transition temperature for the dislocation SLs (within the frame of each SL type).

Magnetic superlattices. The magnetic superlattices consist of alternating layers of materials differing in magnetic properties. Of a particular interest are the SLs with ferromagnetic layers. Such structures provide an additional magnetic modulating potential for the charge carriers but also offer a unique opportunity for fundamental studies of interaction between the magnetic layers through the nonmagnetic spacers. The discovery of exchange layer interaction (ELI) in Fe/Cr/Fe sandwiches [17] has impulsed strongly the investigations in sandwich structures consisting of different ferromagnetic metals separated by nonmagnetic spacers. The ordering of their magnetization in parallel or antiparallel manner was explained well by the quantum interference of conductivity electrons [18]. As to semiconductor systems, the possibility of such an interaction was not studied up to now, because it was thought to be hardly probable due to low concentrations of charge carriers. The SLs of chalcogenide semiconductors offer a unique opportunity for such investi-

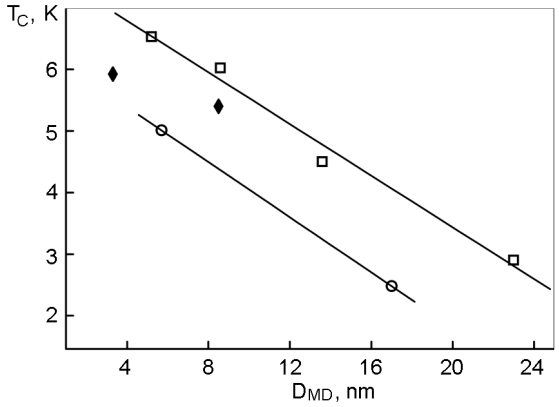

Fig. 7. Dependences of the critical SC transition temperature on the MD network period for SLs of narrow-band semiconductors (□), of combined narrow- and wideband semiconductors (♦) and for SL with ferromagnetic EuS layers (○).

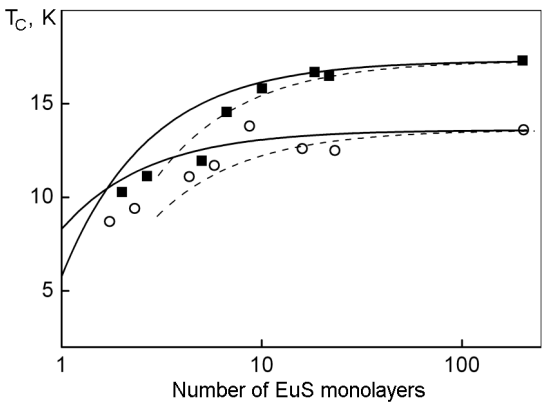

Fig. 8. Dependences of Curie point on the EuS layer thickness for EuS–PbS/(111)BaF2 (○) and EuS–PbS/(001)KCl (■) SLs. Solid lines present the calculated dependences for sharp interphase boundaries; dashed lines, for about 2 monolayers thick intermixed zones at the interphase boundaries.

gations because those include ferromagnetic materials (EuS, EuSe).

First of all, studied were the presence and features of the transition of EuS layers in the SL composition into the ferromagnetic state that was determined from temperature dependences of magnetization and magnetic susceptibility. It has been found [19] that as the EuS thickness is reduced from 10 monolayers to 2 ones, the Curie point drops from 17 K to 9 K (Fig. 8) that is explained by reducing number of nearest magnetic neighbors (Eu ions). Moreover, the Curie point decrease by 2–3 K was revealed due to thermally induced stresses in the film/substrate system caused by difference in the heat expansion coefficients thereof.

The magnetic anisotropy is another important characteristic of the magnetic layers. Proceeding from angular and temperature dependences of the ferromagnetic resonance lines, the magnetic anisotropy constants (K_{EuS}) have been determined for SLs on BaF_2 substrates ($K_v = -0.71$ MJ/m^3 and $K_s = 0.08$ mJ/m^2) and on KCl ones ($K_v = -0.67$ MJ/m^3 and $K_s = 0.05$ mJ/m^2) [20]. The dependence of K_{EuS} on the thickness of layers (d_{EuS}) has been established to correspond to the known relationship $K(d_{EuS}) = K_V + 2K_S/d_{EuS}$ with dominating part of the volume component K_V (form anisotropy), resulting in the magnetization in the EuS layer plane. Using the polarized neutron diffraction, the magnetic anisotropy in the plane of SL layers has been found and the features of the domain structure thereof have been determined. The domain magnetizations in the EuS–YbSe and EuS–PbS SLs have been shown to be oriented along different directions in the layer plane, namely, along the easy axes <110> and <210>, respectively [21].

The neutron diffraction is the most effective method to investigate the magnetic SLs that makes it possible to study the exchange interaction of the magnetic layers and to distinguish the antiferromagnetic (AFM) and ferromagnetic (FM) coupling of neighboring layers. The diffraction patterns have been obtained for EuS–PbS and EuS–YbSe SLs (Fig. 9) where the AFM peaks were observed [22–25]. This allowed to state definitely the AFM coupling (when the magnetization in the neighboring EuS layers is directed oppositely). Such coupling is observed for an unusually large thickness range of the narrow-band semiconductor (PbS) spacers (0.4 to 40 nm) and the wideband (YbSe) one (1 to 3 nm), what is a substantial distinction between the semiconductor SLs and the metallic ones.

A magnetic field applied along the SL layers rotates the magnetization of all the layers to one and the same direction, thus causing the AFM peak disappearance and appearance of a ferromagnetic component in the sites of structure peaks. The switching-off of the external magnetic field restores the AFM ordering of the magnetic layers, so the AFM peaks appear again in the neutron diffraction patterns. Thus, the control of magnetization ordering in neighboring EuS layers in the SLs and triggering thereof out of AFM to FM and vice versa using relatively weak magnetic fields provides very

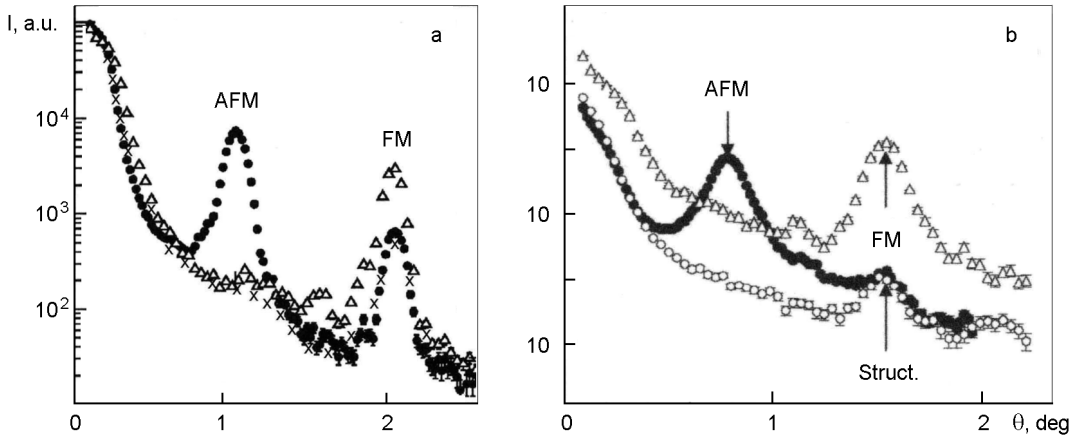

Fig. 9. Neutron diffraction patterns for EuS(4.4 nm)–YbSe(2 nm)/(001)KCl (a) and EuS(6 nm)–PbS(2.3 nm)/(001)KCl (b) SLs at T = 35 K, B = 0 Gs (○,×), T = 4.3 K, B = 0 Gs (●) and T = 4.3 K, B = 185 Gs (Δ).

good promises for such structures in the spintronics (spin-polarized electronics) making it possible to control not only the charge carrier current but the spin state thereof.

It is to note that none of modern theoretical models is able of explanation of the observed experimental results.

Thus, the use of multilayer films with large misfit ranges in the layer lattice parameters makes it possible not only to extend substantially the range of potential superlattice materials but also to provide one-, two-, and three-dimensional superlattice nanostructures with new unique optical, electrical, and magnetic properties.

The work was supported financially by CRDF Grant # UKP2-2896-KV-07.

References

1. L.Esaki, R.Tsu, *IBM J. Res. Dev.*, **14**, 61 (1970).
2. L.S.Palatnik, A.I.Fedorenko, *J. Cryst. Growth*, **52**, 917 (1981).
3. A.Fedorov, A.Sipatov, V.Volobuev, *Thin Solid Films*, **425**, 287 (2003).
4. A.G.Fedorov, I.A.Shneiderman, A.Yu.Sipatov et al., *J. Cryst. Growth*, **198/199**, 1211 (1999).
5. A.G.Fedorov, A.Yu.Sipatov, E.V.Kaidalova, *Functional Materials*, **6**, 860 (1999).
6. I.V.Kolesnikov, A.Yu.Sipatov, *Sov. Phys. Semicond.*, **23**, 598 (1989).
7. K.H.Herrmann, J.Auth, K.P.Mollmann et al., *Semicond. Sci. and Technol.*, **8**, 176 (1993).
8. A.Yu.Sipatov, *Low Temp. Phys.*, **25**, 376 (1999).
9. V.N.Lutskii, V.A.Petrov, A.S.Rylik et al., *Phys. Low-Dim. Struct.*, **7**, 37 (1994).
10. M.Figielski, A.Morawski, T.Wosinski et al., *J. Superconductivity: Incorpor. Nov. Magn.*, **16**, 183 (2003).
11. S.Wrotek, K.Dybko, A.Morawski et al., *Acta Phys. Pol.*, **A 103**, 629, (2003).
12. O.A.Mironov, B.A.Savitsky, A.Yu.Sipatov et al., *Zh.Eksp.Teor.Fiz. Lett.*, **48**, 106 (1988).
13. N.L.Bobrov, L.F.Rybalchenko, V.V.Fisun et al., *Fiz. Nizk. Temp.*, **16**, 1531 (1990).
14. N.Y.Fogel, A.I.Erenburg, A.Pokhila et al., *Physica B*, **284–288**, 1123 (2000).
15. N.Ya.Fogel, A.S.Pokhila, Yu.V.Bomze et al., *Phys. Rev. Letters*, **86**, 512 (2001).
16. N.Ya.Fogel, E.I.Buchstab, Yu.V.Bomze et al., *Phys. Rev. B*, **66**, 174513 (2002).
17. P.Grunberg, R.Schereiber, Y.Pang et al., *Phys. Rev. Lett.*, **57**, 2442 (1986).
18. P.Bruno, *Phys. Rev. B*, **52**, 411 (1995).
19. A.Stachow-Wojcik, T.Story, W.Dobrowolski et al., *Phys. Rev. B*, **60**, 15220 (1999).
20. T.Story, C.H.W.Swuste, H.J.M.Swagten et al., *Acta Phys. Polonica*, **A97**, 435 (2000).
21. H.Kepa, C.F.Majkrzak, A.Yu.Sipatov, *Physica B*, **345**, 193 (2004).
22. H.Kepa, J.Kutner-Pielaszek, J.Blinowski, *Europhys. Lett.*, **56**, 54 (2001).
23. H.Kepa, P.Sankowski, P.Kacman et al., *J. Magn. Magn. Mater.*, **272–276**, 323 (2004).
24. H.Kepa, C.F.Majkrzak, A.Yu.Sipatov et al., *J. Magn. Magn. Mater.*, **310**, 2280 (2007).
25. H.Kepa, C.F.Majkrzak, A.Sipatov et al., *J.Phys. Condens. Matter.*, **21**, 124207 (2009).

Надграткові наноструктури на основі халькогенідних напівпровідників

О.Ю.Сіпатов

Показано, що використання багатошарових плівок халькогенідних напівпровідників з невідповідністю граток суміжних шарів у широких межах (0,5–13 %) відкриває нові можливості для створення одно-, дво- та тривимірних надграткових наноструктур. Для двовимірних (дислокаційних) надграток вперше виявлено надпровідність, пов'язану з присутністю періодичних сіток дислокацій невідповідності на міжфазних межах. Для тривимірних надграток PbSe–PbS вперше знайдено спектри люмінесценції з квантових точок, утворених модуляцією структури періодичними дислокаціями у площині композиції та модуляцією складу в ортогональному напрямку. Для одновимірних (композиційних) надграток виявлено резонансне тунелювання електронів через феромагнітні бар'єри EuS, а також антиферомагнітне упорядкування магнітних шарів, зумовлене їх взаємодією через діамагнітні прошарки PbS та YbSe. Таке упорядкування спостерігається для незвично великого діапазону товщини прошарків вузькозонного напівпровідника PbS (від 0,4 до 40 нм) та широкозонного YbSe (від 1 до 3 нм).